

This item was submitted to [Loughborough's Research Repository](#) by the author.
Items in Figshare are protected by copyright, with all rights reserved, unless otherwise indicated.

Interactions between tribology and dynamics of automotive differential hypoid gears considering thermal non-newtonian mixed lubrication effects

PLEASE CITE THE PUBLISHED VERSION

PUBLISHER

5th World Tribology Congress

VERSION

AM (Accepted Manuscript)

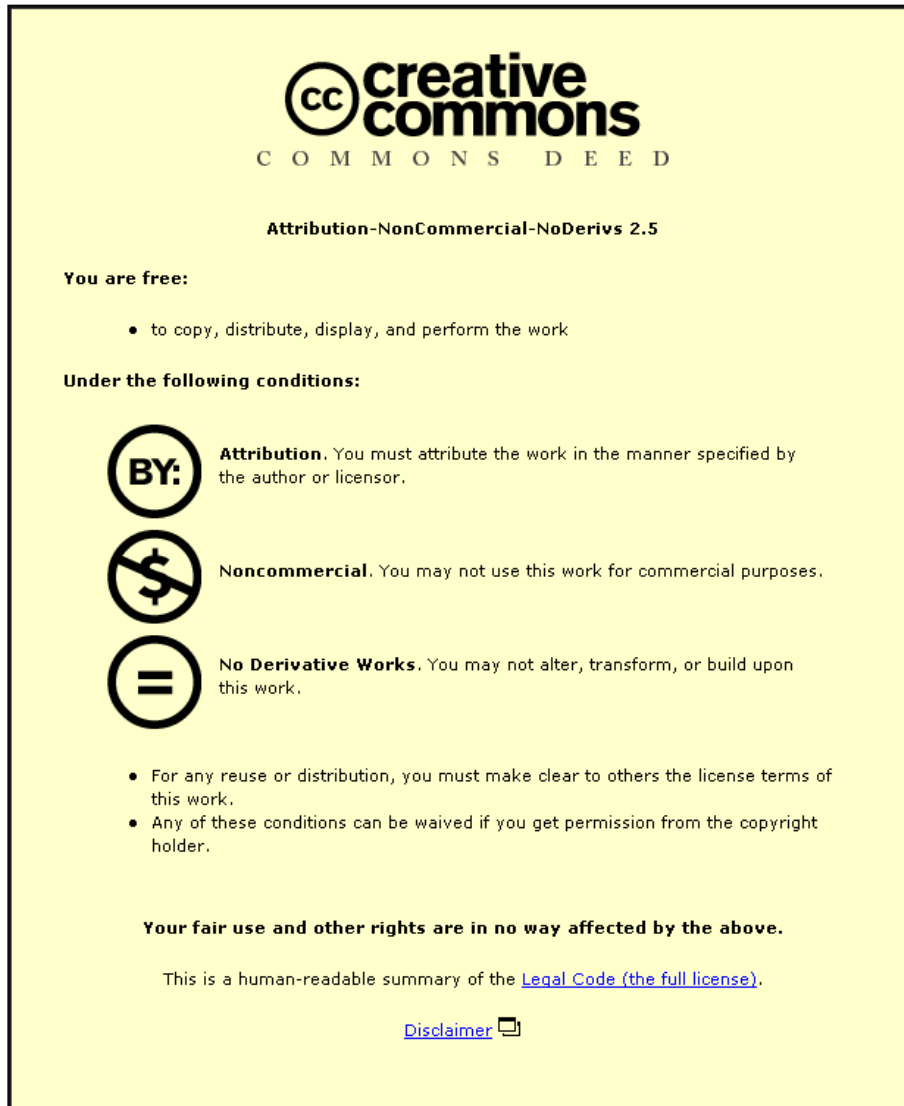
LICENCE

CC BY-NC-ND 4.0

REPOSITORY RECORD

Mohammadpour, Mahdi, Stephanos Theodossiades, and Homer Rahnejat. 2019. "Interactions Between Tribology and Dynamics of Automotive Differential Hypoid Gears Considering Thermal Non-newtonian Mixed Lubrication Effects". figshare. <https://hdl.handle.net/2134/14264>.

This item was submitted to Loughborough's Institutional Repository (<https://dspace.lboro.ac.uk/>) by the author and is made available under the following Creative Commons Licence conditions.



CC creative commons
COMMONS DEED

Attribution-NonCommercial-NoDerivs 2.5

You are free:

- to copy, distribute, display, and perform the work

Under the following conditions:

BY: **Attribution.** You must attribute the work in the manner specified by the author or licensor.


Noncommercial. You may not use this work for commercial purposes.

No Derivative Works. You may not alter, transform, or build upon this work.

- For any reuse or distribution, you must make clear to others the license terms of this work.
- Any of these conditions can be waived if you get permission from the copyright holder.

Your fair use and other rights are in no way affected by the above.

This is a human-readable summary of the [Legal Code \(the full license\)](#).

[Disclaimer](#) 

For the full text of this licence, please go to:
<http://creativecommons.org/licenses/by-nc-nd/2.5/>

Interactions between Tribology and Dynamics of Automotive Differential Hypoid Gears Considering Thermal Non-Newtonian Mixed Lubrication Effects

Mahdi Mohammadpour^{1)*}, Stephanos Theodossiades²⁾ and Homer Rahnejat²⁾

¹⁾ Wolfson School of Mechanical and Manufacturing Engineering, Loughborough University, Loughborough, UK

*Corresponding author: m.mohammad-pour@lboro.ac.uk

1. Introduction

One of the key design targets for differential hypoid gears is improved efficiency, which depends critically on the formation of a lubricant film. Therefore, tribological predictions are essential in order to study parasitic losses. Another key parameter in gear design is dynamics performance and thus noise, vibration and harshness (NVH). Various researchers have investigated the dynamics of non-parallel axes gears, such as hypoid and bevel gears [1-4]. EHL of hypoid gear pairs has also been investigated in [5, 6]. However, in these works the quasi-static calculations have neglected the gear dynamic behavior. Tooth contact analysis (TCA) has been used to provide the necessary input for the EHL models.

The current work shows that gear dynamics and contact tribology are inexorably linked, and therefore, need to be integrated as follows:

1. With regard to dynamic modeling, the stiffness and damping of the lubricant film are important parameters. This link establishes the first relationship between dynamics and tribology of hypoid gears.
2. Viscous shear of the lubricant in meshing teeth pairs also dissipates some of the input energy and thus is a source of damping itself. This is the second relationship between dynamics and tribology of hypoid gears. Thermal non-Newtonian behavior would be mostly encountered.
3. On the other hand, in order to undertake tribological assessment realistic contact loads and speed of lubricant entraining motion is required for any instantaneous contact. In the case of hypoid gears pairs, a quasi-static solution cannot provide suitable estimates of these parameters as inertial effects are not taken into account nor the continuity of time history of motions is considered. This linkage forms the third relationship between dynamics and tribology for gearing systems.

The stiffness of the lubricant film depends on its rheological state under the prevailing dynamic conditions. At relatively low loads, a hydrodynamic regime of lubrication may be prevalent and the lubricant film may be regarded as compressible. This means that lubricant film stiffness can be the determining factor in the overall contact stiffness. The compressibility of the lubricant under hydrodynamic conditions can also result in a modest contribution to system damping. At high loads, elastohydrodynamic regime of lubrication is prevalent, where the lubricant film is regarded as incompressible. The amorphous nature of the lubricant in the contact under EHL conditions presents insignificant damping [7] and relatively high stiffness in such a way that a dry elastostatic Hertzian contact may be assumed in any suitable quasi-static step-wise analysis.

Some extrapolated/empirical equations to estimate friction and film thickness have been reported. Also, there are some suitable formulae for application of friction to the case of hypoid gear teeth pairs. The first equation for film

thickness was provided in a paper on EHL by Grubin [8], based on the work of Ertel [9]. In fact, Grubin presented an equation based on his analytical solution of circular point contact EHL. The equation takes into account the effect of contact load, surface velocities and lubricant rheological parameters; viscosity and pressure-viscosity coefficient. However, it ignores the side leakage from the contact described by Gohar [10]. Mostofi and Gohar [11] provided numerical predictions, as well as extrapolated film thickness equations for both the central flat and the minimum exit constriction films. Furthermore, for the first time they included the effect of squeeze film action in their numerical analysis. Their equation takes into account the angled flow and also covers the side leakage, but does not show the same trend for film thickness variation in a meshing cycle [5]. After original contribution of Mostofi and Gohar [11], Chittenden et al [12] provided extrapolated oil film thickness formulae with angled flow.

In hypoid gear applications, the contact is mostly a long ellipse with a large ellipticity ratio and with angled flow. Chittenden's equation [12] can simulate all these conditions and is extrapolated for similar load, speed, material and geometrical combination of the current study. It shows good agreement with numerical modeling of EHL contacts in hypoid gear pairs [5].

Based on [13], thermal effects on EHL film thickness are negligible despite the significant effect on friction. It is also claimed in [14] that non-Newtonian effects show same behavior with thermal effects on film thickness and friction. Therefore, the isothermal Newtonian form of Chittenden equation is suitable for the analysis in this work.

This paper presents an investigation into Elastohydrodynamic (EHL) or Hydrodynamic modeling of differential hypoid gear teeth contacts, coupled with multi-body dynamics to study the dynamics and efficiency of gear pairs.

A multi-body model of hypoid gears with torsional degrees of freedom has been developed. In the EHL regime of lubrication this model calculates teeth pair contact reactions from their dynamic response and neglects the stiffness and damping coefficients of the lubricant film, as previously justified. Friction and the required film thickness are calculated using available extrapolated equations.

Then, the EHL model predicts the film thickness and power loss in a quasi-static manner at some snapshots during a typical meshing cycle. A numerical model of EHL elliptical point contact is presented in order to obtain the film behavior under the usual range of operating conditions of vehicle differential hypoid gear pairs, taking into account non-Newtonian thermal shear. Distributed line low relaxation effective influence Newton-Raphson method is used for rapid numerical convergence [5]. In the case of highly loaded contacts, usually a thin film yields mixed regime of lubrication. In such cases the effect of boundary friction should be considered.

Lightly loaded hydrodynamic condition usually takes place when the load is very low or teeth separation occurs. Teeth separation is one of the main causes of NVH problems, also considered to be responsible for axle whine noise. In this condition, the gap between teeth flank pairs is calculated using rigid multi-body analysis. In this case the applied contact load is obtained after the lubricant reaction is calculated from multi-body model that to be applied on the torsional system. Therefore, an iterative solution between tribology and multi-body dynamics model is required. In current study, only highly loaded condition is studied and the lubrication regime is always EHL.

2. Tribological Model

As it is mentioned above, in the current study conditions that lead to the EHL regime of lubrication are considered. Therefore, the dominant stiffness and damping are those of the bounding solids in accord with Hertzian condition, not those of the lubricant. This means the dynamic model can be used without obtaining the stiffness and damping from the tribological model.

An analytical-experimental equation for the calculation of coefficient of friction is presented in [15], considering the non-Newtonian behavior of the thin lubricant film and thermal effects:

$$\mu = 0.87\alpha\tau_0 + 1.74\frac{\tau_0}{\bar{p}} \ln\left(\frac{1.2}{\tau_0 h_{c0}} \left(\frac{2k\eta_0}{1+9.6\zeta}\right)^{1/2}\right) \quad (1)$$

where:

$$\zeta = \frac{4}{\pi} \frac{K}{h_{c0}/R'} \left(\frac{\bar{p}}{E'R'K'\rho'c'U'}\right)^{1/2} \quad (2)$$

To calculate boundary friction, the presented method in [16] is used. This model assumes a Gaussian distribution of asperity heights with a mean radius of curvature for an asperity summit. A full procedure for this method is provided in [5].

Film thickness, h is required for the calculation of friction and is estimated using Chittenden's extrapolated oil film thickness formula [12] for elliptical point contacts with angled lubricant flow entrainment into the conjunction:

$$h_{c0}^* = 4.31U^{*0.68}G^{*0.49}W^{*0.073} \left\{1 - \exp\left[-1.23\left(\frac{R_s}{R_e}\right)^{2/3}\right]\right\} \quad (3)$$

where, the non-dimensional groups are:

$$W^* = \frac{\pi F_{fl}}{2E_r R_e^2} \quad U^* = \frac{\pi\eta_0 U'}{4E_r R_e} \quad G^* = \frac{2}{\pi}(E_r \alpha)$$

and

$$\frac{1}{R_e} = \frac{\cos^2\theta}{R_{zx}} + \frac{\sin^2\theta}{R_{zy}}, \quad \frac{1}{R_s} = \frac{\sin^2\theta}{R_{zx}} + \frac{\cos^2\theta}{R_{zy}}$$

After simulation runs of the dynamic model with the empirical tribological model, the operating conditions for a complete meshing cycle are obtained and detailed numerical EHL analysis is used quasi-statically to calculate film and generated pressures. Owing to insignificant effects of thermal and non-Newtonian behavior on film thickness, an isothermal Newtonian approach [5] is utilized.

3. Dynamic Model

The multi-body model comprises a two-degree of freedom torsional model developed in ADAMS

environment. The governing equations of motion have been presented below. The indices p and g refer to the pinion and gear, respectively. Same methodology has been used by Karagiannis et al. [17]. The mesh stiffness variation with respect to pinion angle $k_m(\varphi_p)$ has been calculated using TCA analysis [17]. 3% damping ratio has been used for the calculation of damping coefficient, c_m .

$$\begin{aligned} I_p \ddot{\varphi}_p + R_p c_m \dot{x} + R_p k_m(\varphi_p) f(x) &= T_p + T_{fr,p} \\ I_g \ddot{\varphi}_g - R_g c_m \dot{x} - R_g k_m(\varphi_p) f(x) &= -T_g + T_{fr,g} \end{aligned} \quad (4)$$

To take into account for contact/impact and separation, the following equation is included:

$$f(x) = \begin{cases} x-b, & x \geq b \\ 0, & -b < x < b \\ x+b, & x \leq -b \end{cases} \quad (5)$$

To include the road conditions and variations of the resisting wheels' torque with velocity, this is calculated considering the tire rolling resistance and aerodynamic resistance [18] as:

$$T_g = Fr_{wheel} \quad (6)$$

where:

$$F = ma + R_a + R_{rl} + R_{gr}$$

$$R_a = \frac{\rho}{2} C_D A_f V^2$$

$$R_{rl} = f_{rl} W$$

$$f_{rl} = 0.01 \left(1 + \frac{V}{147}\right)$$

The input torque to the differential includes the sinusoidal variation in engine torque (engine order vibration [19]):

$$T_p = \frac{R_p}{R_g} T_{g0} (1 + 0.1 \cos(2R_t A_p)) \quad (7)$$

The frictional torque in gear teeth meshing is given as:

$$\begin{aligned} T_{fr,p} &= R_p f r \\ T_{fr,g} &= R_g f r \\ f r &= W_n \mu \end{aligned} \quad (8)$$

In these set of equations the key point is the coefficient of friction (presented in previous section).

4. Results and Discussion

The hypoid gear pair of a commercial vehicle is considered in the current analysis. The related gear data are listed in Table 1. Table 2 lists the vehicle data, which determine the resisting torque on the gear side at any speed. Required rheological data and thermal properties of lubricant are presented in Table 3.

The studied cases lead to continuous meshing conditions without teeth pair separations. These conditions pertain to teeth pair contact, subjected to the EHL regime of lubrication. Therefore, the dynamic model can be simulated with the previously stated empirical equations. Once dynamic analysis is carried out, flank load, surface speed and geometry are determined. Figure 1 shows the flank load during some meshing cycles. In this figure, it is clear that the expected flank load (contact force per meshing teeth pair) is in the range of several kN (highly loaded conditions).

Using the above stated outputs of the dynamic model, a full numerical model of EHL contact is used for quasi-static contact calculations. This gives detailed results of film thickness and pressure distribution for engaged meshing gear teeth. Figure 2 shows a snapshot of the elastohydrodynamic pressure distribution. The maximum pressure is approximately 1 GPa.

Table 1: Gear pair parameters

Parameter name	pinion	gear
Number of teeth	13	36
face-width (mm)	33.851	29.999
face angle (deg)	29.056	59.653
pitch angle (deg)	29.056	59.653
root angle (deg)	29.056	59.653
spiral angle (deg)	45.989	27.601
pitch apex (mm)	-9.085	8.987
face apex (mm)	1.368	10.948
Outer cone distance (mm)	83.084	95.598
offset (mm)	24.0000028	24
Hand	Right	Left

Table 2: Analysis conditions

Parameter name	value
A_f (frontal area)	3.42 m ²
f_r (rolling resistance coefficient)	0.0166
C_D (drag coefficient)	1.15
ρ (air density)	1.22 kg/m ³
W (vehicle weight)	2340 kg
Tire	P205/65R15 BSW
2nd gear ratio	1.5:1
Surface Roughness of solids	0.5 μ m

Table 3: Lubricant and solids properties

Pressure viscosity coefficient (α)	2.3827E-008 [Pa-1]
Atmospheric dynamic viscosity @ 40°C (η_0)	0.19514 [Pa.s]
Atmospheric dynamic viscosity @ 100°C (η_0)	0.0170304 [Pa.s]
Eyring stress τ_0	2 [MPa]
τ_{L0}	2.3 [MPa]
Pressure-induced shear coefficient (λ')	0.08
Thermal conductivity of fluid	0.14 [J/kgK]
Heat capacity of fluid	2000 [W/mK]
Modulus of elasticity of contacting solids	210 [GPa]
Poisson's ratio of contacting solids	0.3 [-]
Density of contacting solids	7850[kg/m ³]
Thermal conductivity of contacting solids	46 [W/mK]
Heat capacity of contacting solids	470 [J/kgK]

Figure 3 illustrates the variation of minimum film thickness during few meshing cycles. It shows that film thickness is estimated to be of the order of a few tenths of micrometer. This means that a mixed regime of lubrication would be expected. Using the calculated pressure distribution and film thickness, lubricant shear stress can be calculated. Its integration over the contact footprint yields the value of friction. The transmission inefficiency is defined as:

$$\varepsilon = \frac{\sum P_{fj}}{T\omega} \times 100 \quad (9)$$

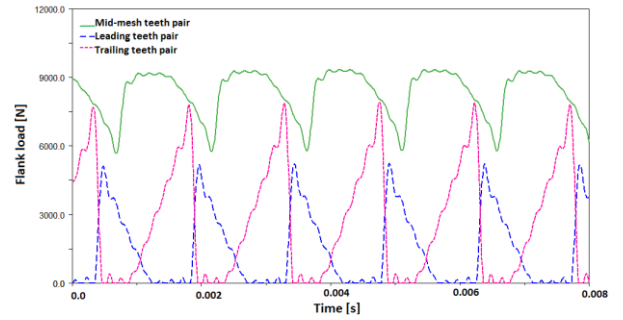


Figure 1. Flank load for one complete cycle

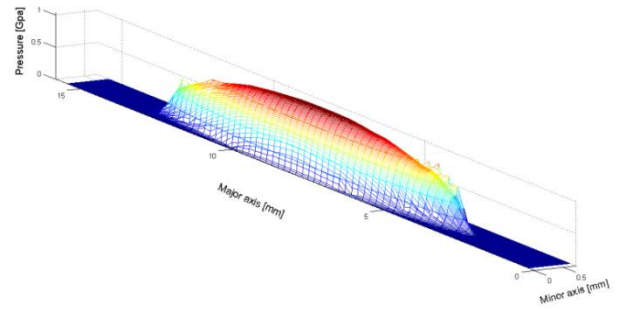


Figure 2. Pressure distribution for one snapshot of the meshing cycle

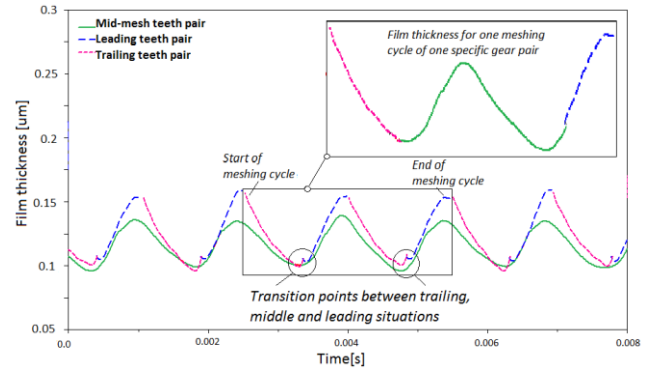


Figure 3. Film thickness for one complete cycle

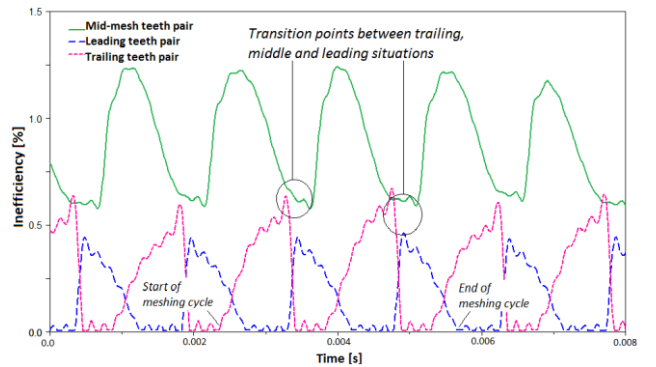


Figure 4. Teeth Inefficiency for one complete cycle

Where $P_{fj} = f_{rj}\Delta u_j$ is the frictional power loss, Δu_j is the sliding velocity of teeth pairs j , while T and ω are the pinion torque and angular velocity, respectively. Figure 4 shows the variation of inefficiency during a few meshing cycles. It shows that inefficiency of the studied hypoid gear pair under the considered conditions has a maximum value

of 1.2%.

5. Concluding Remarks

Two key points in hypoid gears design are NVH refinement and efficiency. In order to estimate and refine these parameters a coupled solution between dynamics and tribology is required. Integration between dynamics and tribological models are through stiffness and damping of the lubricant film, flank friction and the effect of dynamic loads in an iterative process.

6. Nomenclature

A_f	Vehicle frontal area
A_p	Pinion angle
a	Acceleration
b	Half of teeth pair backlash
c_m	Damping coefficient in the direction of mesh
c'	Thermal coefficient of bounding solid surfaces
E_r	Reduced elastic modulus
$\pi / \left(\frac{1 - \nu_p^2}{E_p} \right) + \left(\frac{1 - \nu_w^2}{E_w} \right)$	
E_w, E_p	Young's modulus of gear and pinion material
E'	E_r / π
F	Traction
h_{c0}	Central contact film thickness
h_m	Minimum film thickness
h^*	Dimensionless film thickness
I_p, I_g	mass moments of inertia of pinion and gear
\bar{K}	Thermal conductivity of the lubricant
K'	Thermal conductivity of the solids
k_m	mesh stiffness
m	Vehicle mass
T_p, T_g	externally applied torques to the pinion and gear
$T_{fr,p}, T_{fr,g}$	frictional moments at pinion and gear
\bar{p}	Average pressure
R_{zx}	Equivalent radius of contact along the minor axis
R_{zy}	Equivalent radius of contact along the major axis
R'	Equivalent radius
R_p, R_g	pinion and gear contact radii
R_a	Aerodynamic resistance
R_{rl}	Rolling resistance
R_{gr}	Gravitational resistance
R_t	Transmission ratio
r_{wheel}	Tire radius
U	Speed of entraining motion
V	Vehicle speed
W_n	Calculated contact load
α	Lubricant pressure-viscosity coefficient
μ	Coefficient of friction
η_0	Lubricant dynamic viscosity
θ	Angle of lubricant entrainment into the contact
ν_p	Poisson's ratio for the pinion gear material
ν_w	Poisson's ratio for the gear wheel material
ρ'	Density of solids
τ_0	Eyring shear stress
φ_p, φ_g	pinion and gear angle of rotation
ω_{mesh}	meshing frequency

7. References

[1]Kolivand, M. and Kahraman, A. "A load distribution

model for hypoid gears using ease-off topography and shell theory", *Mechanism & Machine Theory*, 2009, 44, pp. 1848–1865

[2]Xu, H. and Kahraman, A. "Prediction of friction-related power losses of hypoid gear pairs", *Proc. Instn. Mech. Engrs, J. Multi-body Dyn.*, 2007, 221, pp. 387-400

[3]Cheng, Y. and Lim, T.C., "Vibration analysis of hypoid transmission applying an exact geometry based gear mesh theory", *Journal of Sound and Vibration*, 2001, 240(3), pp. 519-543

[4]Wang, J., Lim, T.C. and Li, M., "Dynamics of a hypoid gear pair considering the effects of time-varying mesh parameters and backlash nonlinearity", *Journal of Sound and Vibration*, 2007, 229(2), pp.287-310.

[5]Mohammadpour, M. Theodossiades, S. and Rahnejat, H. "Elastohydrodynamic lubrication of hypoid gears at high loads", *Proc. IMechE., Part J: J. Engng. Tribology*, 2012, 226

[6]Simon, V. "Head-cutter for optimal tooth modifications in spiral bevel gears", *Mech. & Mach. Theory*, 44, 1420–1435 (2009)

[7]Mehdigoli, H., Rahnejat, H. and Gohar, R. "Vibration response of wavy surfaced disc in elastohydrodynamic rolling contact", *Wear*, 139(1), 1990, pp. 1-15

[8]Ertel, A.N. "Hydrodynamic lubrication based on new principles", *Akad. Nauk. SSSR. Prikadnaya Matematika i Mekhanika*, 3(2), 41-52 (1939)

[9]Grubin, A.N. "Contact stresses in toothed gears and worm gears", *Book 30 CSRI for Technology and Mechanical Engineering*, Moscow, DSRI Trans., 337 (1949)

[10]Gohar, R. *Elastohydrodynamics*, Imperial College Press, London (2001)

[11]Mostofi, A. and Gohar, R. "Oil film thickness and pressure distribution in elastohydrodynamic point contacts", *Proc. Instn. Mech. Engrs., J. Mech. Engng. Sci.*, 24, 171-182 (1982)

[12]Chittenden, R. J., Dowson, D., Dunn, J. F. and Taylor, C. M. "A theoretical analysis of the isothermal elastohydrodynamic lubrication of concentrated contacts. II. General Case, with lubricant entrainment along either principal axis of the Hertzian contact ellipse or at some intermediate angle", *Proc. Roy. Soc., Ser. A*, 397, 271-294 (1985)

[13]Yang, P., Cui, J., Jin, Z. M., Dowson, D., "Transient elastohydrodynamic analysis of elliptical contacts. Part 2: thermal and Newtonian lubricant solution", *Proc. IMechE, Part J: J. Engineering Tribology*, 2005, 219, 187–200

[14]Kim, K. H. and Sadeghi, F. "Non-Newtonian elastohydrodynamic lubrication of point contacts.", *Trans. ASME, J. Trib.*, 113, 1991, pp. 703-711

[15]Evans, C. R. and Johnson, K. L. "Regimes of traction in elastohydrodynamic lubrication", *Proc. Instn. Mech. Engrs.*, 1986, 200 (C5), pp. 313–324

[16]Greenwood, J. A. and Tripp, J. H. "The contact of two nominally flat rough surfaces", *Proc. Instn. Mech. Engrs*, 1970-71. 185, pp. 625-633

[17]Karagiannis, Y., Theodossiades, S. and Rahnejat, H. "On the dynamics of lubricated hypoid gears", *Mechanism & Machine Theory*, 2012, 48, pp. 94-120

[18]Gillespie, T. D. *Fundamentals of Vehicle Dynamics*, Society of Automotive Engineering, Inc. Pa, USA, 1992

[19]Rahnejat, H., *Multi-body dynamics: Vehicles, Machines and Mechanisms*, Professional Engineering Publishing (IMechE), Bury St Edmunds, 1998